



**University of  
Zurich**<sup>UZH</sup>

**Zurich Open Repository and  
Archive**

University of Zurich  
University Library  
Strickhofstrasse 39  
CH-8057 Zurich  
[www.zora.uzh.ch](http://www.zora.uzh.ch)

---

Year: 2015

---

## **ARTD1-induced poly-ADP-ribose formation enhances PPAR ligand binding and co-factor exchange**

Lehmann, Mareike ; Pirinen, Eija ; Mirsaidi, Ali ; Kunze, Friedrich A ; Richards, Peter J ; Auwerx, Johan ; Hottiger, Michael O

**Abstract:** PPAR -dependent gene expression during adipogenesis is facilitated by ADP-ribosyltransferase D-type 1 (ARTD1; PARP1)-catalyzed poly-ADP-ribose (PAR) formation. Adipogenesis is accompanied by a dynamic modulation of the chromatin landscape at PPAR target genes by ligand-dependent co-factor exchange. However, how endogenous PPAR ligands, which have a low affinity for the receptor and are present at low levels in the cell, can induce sufficient co-factor exchange is unknown. Moreover, the significance of PAR formation in PPAR-regulated adipose tissue function is also unknown. Here, we show that inhibition of PAR formation in mice on a high-fat diet reduces weight gain and cell size of adipocytes, as well as PPAR target gene expression in white adipose tissue. Mechanistically, topoisomerase II activity induces ARTD1 recruitment to PPAR target genes, and ARTD1 automodification enhances ligand binding to PPAR, thus promoting sufficient transcriptional co-factor exchange in adipocytes. Thus, ARTD1-mediated PAR formation during adipogenesis is necessary to adequately convey the low signal of endogenous PPAR ligand to effective gene expression. These results uncover a new regulatory mechanism of ARTD1-induced ADP-ribosylation and highlight its importance for nuclear factor-regulated gene expression.

DOI: <https://doi.org/10.1093/nar/gku1260>

Posted at the Zurich Open Repository and Archive, University of Zurich

ZORA URL: <https://doi.org/10.5167/uzh-103773>

Journal Article

Published Version

Originally published at:

Lehmann, Mareike; Pirinen, Eija; Mirsaidi, Ali; Kunze, Friedrich A; Richards, Peter J; Auwerx, Johan; Hottiger, Michael O (2015). ARTD1-induced poly-ADP-ribose formation enhances PPAR ligand binding and co-factor exchange. *Nucleic Acids Research*, 43(1):129-142.

DOI: <https://doi.org/10.1093/nar/gku1260>

# ARTD1-induced poly-ADP-ribose formation enhances PPAR $\gamma$ ligand binding and co-factor exchange

Mareike Lehmann<sup>1,2</sup>, Eija Pirinen<sup>3,4</sup>, Ali Mirsaidi<sup>5,6</sup>, Friedrich A. Kunze<sup>1,2</sup>, Peter J. Richards<sup>5,6</sup>, Johan Auwerx<sup>3</sup> and Michael O. Hottiger<sup>1,5,6,\*</sup>

<sup>1</sup>Institute of Veterinary Biochemistry and Molecular Biology, University of Zurich, 8057 Zurich, Switzerland, <sup>2</sup>Life Science Zurich Graduate School, Molecular Life Science Program, University of Zurich, 8057 Zurich, Switzerland, <sup>3</sup>Laboratory of Integrative and Systems Physiology, Ecole Polytechnique Fédérale de Lausanne, 1015 Lausanne, Switzerland, <sup>4</sup>Biotechnology and Molecular Medicine, A.I. Virtanen Institute for Molecular Sciences, Biocenter Kuopio, University of Eastern Finland, Kuopio, Finland, <sup>5</sup>Competence Centre for Applied Biotechnology and Molecular Medicine, University of Zurich, 8057 Zurich, Switzerland and <sup>6</sup>Zurich Centre for Integrative Human Physiology (ZIHP), University of Zurich, 8057 Zurich, Switzerland

Received September 12, 2014; Revised November 11, 2014; Accepted November 15, 2014

## ABSTRACT

PPAR $\gamma$ -dependent gene expression during adipogenesis is facilitated by ADP-ribosyltransferase D-type 1 (ARTD1; PARP1)-catalyzed poly-ADP-ribose (PAR) formation. Adipogenesis is accompanied by a dynamic modulation of the chromatin landscape at PPAR $\gamma$  target genes by ligand-dependent co-factor exchange. However, how endogenous PPAR $\gamma$  ligands, which have a low affinity for the receptor and are present at low levels in the cell, can induce sufficient co-factor exchange is unknown. Moreover, the significance of PAR formation in PPAR $\gamma$ -regulated adipose tissue function is also unknown. Here, we show that inhibition of PAR formation in mice on a high-fat diet reduces weight gain and cell size of adipocytes, as well as PPAR $\gamma$  target gene expression in white adipose tissue. Mechanistically, topoisomerase II activity induces ARTD1 recruitment to PPAR $\gamma$  target genes, and ARTD1 automodification enhances ligand binding to PPAR $\gamma$ , thus promoting sufficient transcriptional co-factor exchange in adipocytes. Thus, ARTD1-mediated PAR formation during adipogenesis is necessary to adequately convey the low signal of endogenous PPAR $\gamma$  ligand to effective gene expression. These results uncover a new regulatory mechanism of ARTD1-induced ADP-ribosylation and highlight its importance for nuclear factor-regulated gene expression.

## INTRODUCTION

Adipocyte formation relies on the adipogenic differentiation of multipotent mesenchymal stromal cells, resulting in lipid accumulation and which is associated with the capacity to influence numerous biological processes, including signaling and immune functions (1). The underlying mechanism of adipogenesis is a broad reorganization of the transcriptional landscape due to large-scale chromatin changes (2). Instrumental in this step-wise reorganization is the transcription factor peroxisome proliferator-activated receptor gamma (PPAR $\gamma$ ) (3,4) and, in particular, the adipocyte-specific isoform PPAR $\gamma$ 2 (5,6). PPAR $\gamma$  is a nuclear receptor of the PPAR family that functions as an obligate heterodimer with RXRs (7–10). Like many nuclear receptors, PPAR $\gamma$  contains an N-terminal, non-conserved A/B domain, a DNA-binding domain and a C-terminal ligand binding domain (LBD). Hetero-dimerization with RXRs is governed by the C-terminal domain, and ligand binding is conveyed by the LBD, which harbors multiple hydrophobic residues and is important for ligand-dependent interactions with co-factors (11,12). Binding of ligands to PPAR $\gamma$  triggers a conformational switch that exposes a surface that can interact with LXXLL-containing co-activators. Prior to the activation of PPAR $\gamma$  by its ligands, PPAR $\gamma$  is bound to co-repressors that suppress transcription of target genes and which are dislodged upon ligand binding (13). PPAR $\gamma$  is induced during the differentiation of adipocytes and is highly expressed in white and brown adipose tissue (WAT/BAT) (14). A series of transcription factors, in particular, CCAAT/enhancer-binding proteins (C/EBP)  $\beta$  and  $\delta$ , bind to promoter regions of adipogenic genes, establishing so-called transcription factor hotspots that are characterized by open chromatin regions and regulate PPAR $\gamma$ 2 as well as C/EBP- $\alpha$  expression and DNA binding (2,4). To-

\*To whom correspondence should be addressed. Tel: +41 44 635 54 74; Fax: +41 44 635 54 68; Email: hottiger@vetbio.uzh.ch

gether with C/EBP- $\alpha$ , PPAR $\gamma$ 2 determines adipocyte function and transcriptionally co-regulates target genes, such as *adipocyte protein 2* (*aP2*), *cluster of differentiation 36* (*CD36*) and *adiponectin* (15–17).

Polymers of ADP-ribose (PAR) are synthesized by enzymes that belong to the family of ADP-ribosyltransferases (ARTs), which transfer the ADP-ribose moiety of nicotinamide dinucleotide (NAD<sup>+</sup>) to acceptor proteins. Intracellular ADP-ribosylation is catalyzed by the diphtheria toxin-like ADP-ribosyltransferases (ARTDs), which have previously been referred to as poly (ADP-ribose) polymerases (PARPs). Since not all of them catalyze poly-ADP-ribosylation and polymerases refer to enzymes that synthesize DNA/RNA from a template, the new nomenclature has been adopted (18). In humans, ARTDs are currently comprised of 18 members (ARTD1–18), which function in different cellular compartments (18). Of the 18 enzymes, only four have been reported to synthesize PAR (19). The most abundant and so far best-studied PAR-forming member is the chromatin-associated ARTD1 (formerly PARP1), which has been implicated in a plethora of important cellular and biological processes. Thus, ARTD1-dependent poly-ADP-ribosylation has been implicated in the regulation of chromatin compaction, the recruitment of proteins to chromatin, the regulation of enzymatic activities and was described to be involved in biological processes, such as stress signaling, cell death, inflammation, as well as differentiation (20). Furthermore, defects in ADP-ribosylation or in function of ARTDs have been linked to diseases, such as chronic inflammation, neurodegenerative disorders, cardiovascular diseases and cancer (21). Several inhibitors of ADP-ribosylation have been developed, some of which have entered clinical trial (22), and are for historical reasons widely known under the name of PARP inhibitors. Since these inhibitors are not specific for a single ARTD (23), we will simply refer to them as PARP inhibitors and do not adopt a new nomenclature.

We have previously shown that the regulation of PPAR $\gamma$ 2-dependent gene expression and adipocyte function depends on the formation of PAR (24,25). The catalytic activity of ARTD1 is strongly activated during adipogenesis and has been demonstrated to be involved in adipogenesis (24). However, the molecular mechanism that regulates PAR-dependent regulation of PPAR $\gamma$ 2 target gene expression and the functional significance of PAR formation in adipogenesis remained elusive. Moreover, most described endogenous PPAR $\gamma$  ligands show a low affinity for the receptor, and how they induce co-factor exchange at low levels in the cell is currently unknown.

The results presented here confirm that PPAR $\gamma$ -dependent gene expression during adipogenesis depends on PAR formation not only *in vitro* but also *in vivo*. According to our findings, this regulatory function of poly-ADP-ribosylation is brought about by the formation of a complex between ARTD1 and PPAR $\gamma$  at the promoter regions of target genes, a process that increases PPAR $\gamma$  ligand binding and causes the exchange of transcriptional co-repressors, such as nuclear receptor co-repressor (NCoR) with transcriptional co-activators, such as p300. Consistent with this notion, the lack of co-factor exchange in the presence of PARP inhibitors was

overcome by treating the cells with an excess of the PPAR $\gamma$  ligand rosiglitazone. The present study thus elucidates the molecular mechanism by which ARTD1-induced ADP-ribosylation promotes adipogenesis. In addition, the study identifies a new putative role for ARTD1 in the control of ligand-gated transcription factors.

## MATERIALS AND METHODS

### Animal experiments

A novel pan-PARP inhibitor MRLB-45696 (IC<sub>50</sub> for ARTD1 and -2 <1 nM (26)) was kindly provided by Thomas Vogt from Merck Research Laboratories. Ten-week-old male C57BL/6J mice were fed with pellets made in house containing vehicle or PARP inhibitor (50 mg/kg/day) for 18 weeks. All animal experiments were carried out in accordance with the Swiss and EU ethical guidelines and have been approved by the local animal experimentation committee of the Canton de Vaud under license #2465.

### Cell culture

For differentiation, 3T3-L1 cells were plated at 80% confluence, medium was changed after 2 days and induction medium containing 1  $\mu$ g/ml insulin (I-9278), 0.25 mM 3-isobutyl-1-methylxanthine (I-5879) and 0.5  $\mu$ M dexamethasone (D-4902) (Sigma Aldrich, St. Louis, MO, USA) was added after 2 days for three additional days. Starting at day 5, medium was changed every second day to Dulbecco's modified Eagle's medium (DMEM) containing insulin (1  $\mu$ g/ml). Cells were differentiated in the presence or absence of pan-PARP inhibitors PJ34 or ABT888 (both at 1 or 10  $\mu$ M), PARG inhibitor RBPI-3, TopoII inhibitor merbarone (50  $\mu$ M), SIRT1 inhibitor EX527 (10  $\mu$ M) or PPAR $\gamma$  agonist rosiglitazone (1 or 10  $\mu$ M) added to the cells every 24 h. For differentiation until day 21, ABT888 was added only every second day. H<sub>2</sub>O<sub>2</sub> treatment (1 mM, 15 min) was performed in DMEM without fetal calf serum (FCS) (and in the presence of catalase inhibitor 3-AT (30  $\mu$ M) and in the presence or absence of PJ34 (10  $\mu$ M)).

### GST-pulldown

GST-PPAR $\gamma$ 2 was coupled to magnetic GST-Beads (Pierce). Note that 1  $\mu$ g modified or unmodified ARTD1 (in reaction buffer, 5 pmol 40mer DNA,  $\pm$ 10  $\mu$ M NAD<sup>+</sup>, 30 min at 30°C) and 1  $\mu$ g His-p300 were added to the GST-PPAR $\gamma$ 2. Pulldown was performed for 2 h at 4°C in pulldown buffer (50 mM Tris pH 7.5, 150 mM KCl, 5 mM MgCl<sub>2</sub>, 0.2 mM ethylenediaminetetraacetic acid (EDTA), 20% glycerol, 0.1% NP40) in the presence of 10  $\mu$ M PJ34. The beads were washed 3 $\times$  with wash buffer (20 mM Tris pH 7.5, 150 mM KCl, 5 mM MgCl<sub>2</sub>, 0.2 mM EDTA, 10% glycerol, 0.1% Tween).

### Chromatin immunoprecipitation (ChIP)

ChIP was performed as previously described (27). For Re-ChIP experiments, the first ChIP (anti-ARTD1) was eluted twice in 10 mM DTT (30 min, at 30°C), diluted in ChIP



buffer and the second ChIP (anti-PPAR $\gamma$ ) was performed as previously described (27).

### Radioligand binding assay

For saturation binding analysis, baculo purified His-PPAR $\gamma$ 2 (1  $\mu$ g) was incubated at 4°C for 3 h in binding buffer containing 10 mM Tris (pH 8.0), 50 mM KCl, 10 mM DTT with 40 nM  $^3$ H-rosiglitazone (specific activity 46 Ci/mmol) in a final volume of 100  $\mu$ l in the presence or absence of 1000 $\times$  excess of unlabeled rosiglitazone. Bound ligand was separated from free ligand by filtration over GF/C filter and washing filters twice with ice cold binding buffer. Filters were dried and bound radioactivity quantified by liquid scintillation counting. Unspecific binding was determined by adding 40  $\mu$ M of unlabeled rosiglitazone to the reaction. Experiments with ARTD1 were performed by incubating ARTD1 wt or ARTD1 Y907A/C908Y mutant (40 nM) with 100 nM NAD $^+$ , 2 nM DNA at 30°C for 30 min. The reaction was stopped by the addition of 10  $\mu$ M PARPi (ABT888), and after addition of His-PPAR $\gamma$ 2 and 40 nM  $^3$ H-rosiglitazone, binding evaluated as described above. For experiments with free PAR, ARTD1 wt or ARTD1 mutant Y907A/C908Y (40 nM) were incubated with 100  $\mu$ M NAD $^+$ , 2 nM DNA at 30°C for 30 min in binding buffer. ARTD1 was then degraded by Proteinase K over night, followed by inactivation for 10 min at 80°C with PARPi (ABT888 10  $\mu$ M). After addition of His-PPAR $\gamma$ 2 and 40 nM  $^3$ H-rosiglitazone, binding was evaluated as described above.

## RESULTS

### Pan-PARP inhibitor treatment reduces body weight gain, white adipose tissue content and cell size in mice fed with high-fat diet (HFD)

Earlier studies have implicated a function of ADP-ribosylation and, in particular, ARTD1 in adipogenesis and adipocyte function (24,25,28,29). Although the importance of PAR was already described in cells, the physiological relevance of PAR formation *in vivo* has so far not been investigated before. Accordingly, we hypothesized that the inhibition of PAR formation may have beneficial effects on the onset and development of obesity. In order to test this hypothesis, we treated male wild-type (wt) C57BL/6J mice fed with either chow or a HFD for 18 weeks with a recently characterized pan-PARP inhibitor (26). To confirm that PARP inhibitor treatment reduced PAR formation, we measured total ART activity in adipose tissue. As expected, total ART activity was significantly reduced by 35% in both subcutaneous (sc) and epididymal (epi) WAT of PARP inhibitor-treated mice (Supplementary Figure S1A). Overall, vehicle-treated control mice on the HFD presented with a significantly higher body weight gain compared to PARP inhibitor-treated animals (Figure 1A and B), although their food intake was equal (Supplementary Figure S1B). PARP inhibitor-treated animals have been shown to exhibit increased energy expenditure (26). However, body weight of PARP inhibitor-treated mice on HFD was still higher compared to that of those on chow diet, indicating

that increased energy expenditure cannot completely compensate for the increased calorie uptake. Previous observations showed that PAR formation is essential for adipocyte differentiation and function in culture (24,25). We thus hypothesized that adipocyte function was impaired in PARP inhibitor-treated animals and that this contributes to the decreased body weight on HFD. HFD caused a marked increase in the amount of scWAT, while only minor increases were observed in epi and perirenal (peri) WAT, as well as in BAT (Figure 1C and D). However, the increase in HFD-mediated scWAT observed in PARP inhibitor-treated mice was found to be significantly lower as compared to vehicle-treated control mice, while no significant differences were observed between epiWAT, periWAT or BAT (Figure 1D). To test if this PARP inhibitor treatment effect manifested itself in the morphology of scWAT adipocytes, scWAT was isolated, fixed, stained and subjected to quantitative microscopic analysis. Adipocytes from PARP inhibitor-treated mice were significantly smaller than corresponding cells from scWAT of vehicle-treated control animals (Figure 1E). To investigate if also the epiWAT was affected by PARP inhibitor treatment, although the fat pad weight was unchanged, we analyzed adipocyte morphology in epiWAT. In agreement with earlier studies, adipocytes in epiWAT from PARP inhibitor-treated animals were significantly smaller than those from chow-fed mice (25) (Supplementary Figure S1C). To test if the smaller adipocyte size correlated with a change in adipogenic gene expression, a quantitative reverse transcriptase-polymerase chain reaction (qRT-PCR) analysis was performed. Consistent with earlier studies (25), the reduced body weight gain, the reduced expansion of the scWAT after HFD and PARP inhibitor treatment (Figure 1A–E), and the expression of PPAR $\gamma$  target genes *adiponectin*, *aP2* and *CD36* was significantly reduced, whereas the expression of the key adipogenic regulator *PPAR $\gamma$*  itself was unaffected (Figure 1F). In contrast, epiWAT showed impaired *PPAR $\gamma$ 2* gene expression (Supplementary Figure S1D). Expression of the other adipogenic markers *aP2*, *CD36* and *adiponectin* tended also to be down in epiWAT from PARP inhibitor-treated mice (Supplementary Figure S1D). Small adipocytes have often been shown to be associated with low inflammation (30). To test the inflammatory status of the scWAT of PARP inhibitor-treated animals, we analyzed gene expression of the inflammatory mediators *resistin*, *angiotensinogen*, *interleukin 6 (IL6)* and *tumor necrosis factor  $\alpha$  (TNF $\alpha$ )* (Figure 1G). We found expression of *resistin*, *angiotensinogen* and *IL6* to be downregulated, indicating that the general inflammatory status of PARP inhibitor-treated animals is reduced in comparison to vehicle-treated animals. EpiWAT is known to undergo a substantial degree of inflammation upon feeding with a HFD (31). qRT-PCR analysis of this tissue revealed that PARP inhibitor-treatment also generally reduced HFD-induced inflammatory gene expression in epiWAT (Supplementary Figure S1E).

In summary, these results show that ADP-ribosylation mediates obesity, adipocyte hypertrophy and general adipose tissue inflammation in mice fed with a HFD.

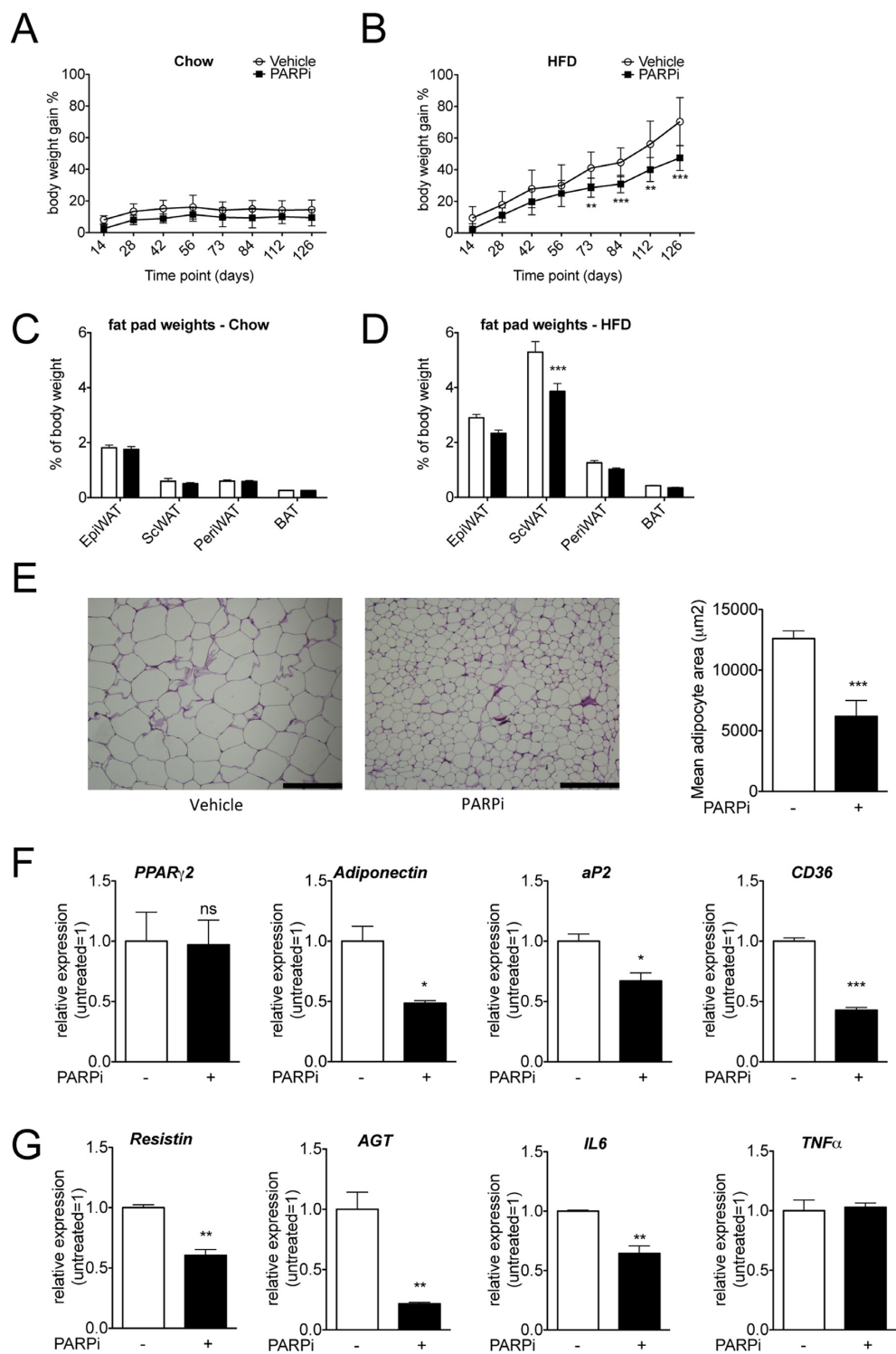


**Figure 1.** PARP inhibitor treatment reduces body weight and adipose tissue size in mice. (A and B) Weight development during chow and HFD in vehicle- and PARP inhibitor-treated mice. Eight-week-old male C57BL/6J mice were fed with chow or HFD containing vehicle (DMSO) or PARP inhibitor (PARPi, 50 mg/kg/day) for 18 weeks. Body weight gain was monitored at the given time points. Two-way ANOVA analysis revealed  $P < 0.001$  for both HFD and chow diet ( $n = 10$ ). (C and D) Fat pad weights on chow and HFD. Animals were sacrificed after overnight fasting using isoflurane inhalation and tissues were collected upon sacrifice and flash-frozen in liquid nitrogen. epiWAT, epididymal white adipose tissue; scWAT, subcutaneous white adipose tissue; periWAT, perirenal white adipose tissue; BAT, brown adipose tissue. Data are mean  $\pm$  SEM. ANOVA one-way test, \*\*\* $P < 0.001$  ( $n = 10$ ). (E) Mouse scWAT was fixed, dehydrated and embedded in paraffin wax. Sequential sections (6  $\mu$ m) were cut and morphological changes visualized using H&E staining (scale bar 200  $\mu$ m). Blinded analysis of mean adipocyte area in tissue sections from mice ( $n = 9$ –10 per treatment group) was performed. (F and G) qRT-PCR analysis of PPAR $\gamma$ -dependent and inflammatory genes of scWAT isolated from vehicle- and PARP inhibitor-treated mice. For qRT-PCR analysis of tissue samples, isolated WAT from 8 mice per group was pooled and expression values were normalized against 36BP4. AGT, angiotensinogen. All data are mean  $\pm$  SEM.  $t$ -Test: \* $P < 0.05$ , \*\* $P < 0.01$ , \*\*\* $P < 0.001$ .

## PAR formation is required for PPAR $\gamma$ -dependent gene expression

To study the mechanistic details of how PAR formation promotes adipogenesis (24), we characterized adipocyte differentiation in 3T3-L1 pre-adipocyte cultures in the presence or absence of different PARP inhibitors. Adipogenesis was induced in 3T3-L1 cells by the addition of insulin, 3-isobutyl-1-methylxanthine (IBMX) and dexamethasone (32), upon which they consistently formed lipid-laden adipocytes (Figure 2A). In line with our earlier studies (24), in which we used the PARP inhibitor PJ34, the presence of the more potent pan-PARP inhibitor ABT888 (which does not inhibit tankyrases) during the first 7 days of adipogenesis strongly reduced the expression of *PPAR $\gamma$ 2* itself and its target genes *aP2*, *CD36* and *adiponectin* (Figure 2B and Supplementary Figure S2A). The inhibitory effect of PARP inhibitors on *PPAR $\gamma$ 2* itself can be explained by our previous results, which showed that PARP inhibitor treatment does not inhibit initial *PPAR $\gamma$ 2* expression, but rather inhibits the regulatory feedback loop of *C/EBP $\alpha$*  and *PPAR $\gamma$*  expression (16,24). To confirm that PAR formation indeed enhances PPAR $\gamma$ -dependent gene expression and adipogenesis, we also performed the reverse experiment and aimed to increase PAR formation by inhibiting PAR degradation with the PARG inhibitor RBPI-3 (Supplementary Figure S2B). In agreement with the hypothesis that PAR formation enhances PPAR $\gamma$ -dependent gene expression, RBPI-3 caused a significant increase in the transcript levels of *PPAR $\gamma$ 2*, *aP2*, *CD36* and *adiponectin* (Figure 2C). Similarly, the inhibition of nicotinamide phosphoribosyltransferase (NAMPT) by FK866, which decreases cellular NAD<sup>+</sup> levels and thus interferes with PAR formation, strongly reduced PPAR $\gamma$ -dependent gene expression and PPAR $\gamma$  protein levels (Supplementary Figure S2C and D). Finally, to rule out that an ARTD family member other than ARTD1 was responsible for the effect of PARP inhibitor treatment, we differentiated ARTD1 knockout and wt mouse embryonic fibroblasts (MEFs) to adipocytes. MEFs lacking ARTD1 did not exhibit detectable PAR formation or induction of PPAR $\gamma$ -dependent gene expression (Supplementary Figure S2E and F), indicating that no other ARTD family member can compensate for the lack of ARTD1 and its enzymatic activity. This is in line with our previous findings that *in vitro* knockdown of ARTD1 in 3T3L1 cells inhibits differentiation (24) and that *in vivo* knockout of ARTD1 in mice on HFD reduces adipogenic gene expression (25). To exclude potential effects on early differentiation events in cell culture (e.g. mitotic clonal expansion), we also treated 3T3-L1 cells with PARP inhibitor only during late stages of adipocyte differentiation, from day 7 to day 21. Again, the PARP inhibitor significantly reduced expression of the PPAR $\gamma$ -dependent genes *aP2*, *CD36* and *adiponectin* (Figure 2D). SIRT1 was described to be a repressor of 3T3-L1 differentiation (33). Both ARTD1 and SIRT1 are NAD<sup>+</sup>-consuming enzymes that compete for the cellular NAD<sup>+</sup> pool. To exclude the possibility that increased availability of NAD<sup>+</sup> and thus activation of SIRT1 was responsible for the PARP inhibitor effect (which could also lead to repression of PPAR $\gamma$ -dependent genes), we also performed experiments with a SIRT1 in-

hibitor (Supplementary Figure S2G). As expected, SIRT1 inhibition increased PPAR $\gamma$ -dependent gene expression. However, PARP inhibitor-dependent repression of PPAR $\gamma$ -dependent genes could not be reversed by co-incubation with the SIRT1 inhibitor. We therefore conclude that PAR formation is indeed required for the expression of PPAR $\gamma$  and PPAR $\gamma$ -dependent genes during the differentiation of 3T3-L1 cells to functional, lipid-laden adipocytes.

## Topoisomerase II activity is required for ARTD1 recruitment to PPAR $\gamma$ target genes

ARTD1 is the main intracellular ART and generally responsible for about 90% of the nuclear PAR formed under normal conditions (34). The stimulation of PPAR $\gamma$ -dependent gene expression upon PARG inhibitor treatment thus hints at a role for ARTD1 and PAR in regulating the promoter activity of PPAR $\gamma$  target genes. We first assessed the interaction of ARTD1 with PPAR $\gamma$  by immunoprecipitation experiments of PPAR $\gamma$  from nuclear extracts of 3T3-L1 cells on day 7 of differentiation. The results show that automodified ARTD1, which is known to appear at day 7 of differentiation (24), was co-precipitated using an anti-PPAR $\gamma$  antibody (Figure 3A). ChIP experiments with anti-ARTD1 antibodies confirmed the recruitment of ARTD1 at the PPAR $\gamma$  response elements (PPREs) of PPAR $\gamma$ -dependent genes, which was strongly reduced upon PARP inhibitor treatment (Supplementary Figure S3A). To further confirm this interaction and to analyze whether ARTD1 and PPAR $\gamma$  interact at the promoter region of the respective target genes, re-ChIP experiments were performed. Chromatin taken from 3T3-L1 cells 7 days after induction of differentiation was first precipitated with an anti-ARTD1 antibody and then with an anti-PPAR $\gamma$  antibody, and the presence of PPAR $\gamma$ -driven *aP2*, *adiponectin* *CD36* promoters were subsequently analyzed by qRT-PCR. As a negative control, the PPAR $\gamma$ -independent promoter of *keratin 19* (*K19*) was analyzed (29,35), which did not show any PPAR $\gamma$  recruitment at day 7 (Supplementary Figure S3B). The tested PPREs of *adiponectin*, *aP2* and *CD36* were all enriched by the re-ChIP treatment (Figure 3B). In contrast, the negative control gene *K19* was not enriched. These results indicate a direct interaction of ARTD1 with PPAR $\gamma$  at the PPREs of at least a subset of PPAR $\gamma$  target genes.

Since the recruitment of ARTD1 was largely dependent on PAR formation (Supplementary Figure S3A and C) and we have previously shown that topoisomerase II (TopoII) activity is required for PAR formation in adipogenesis (24) we wondered if TopoII activity was also required for ARTD1 recruitment to PPAR $\gamma$  target genes. As expected, ChIP experiments revealed the enrichment of TopoII at the PPREs of the PPAR $\gamma$ -dependent genes *aP2*, *adiponectin* and *CD36*, while no significant enrichment at the control gene *K19* was observed (Figure 3C). Additionally, ARTD1 recruitment was strongly dependent on TopoII enzymatic activity since merbarone treatment reduced occupancy of ARTD1 at the tested PPREs as measured by ChIP (Figure 3D). Finally, the co-localization of TopoII and ARTD1 in 3T3-L1 cells (day 7 of adipogenesis) was confirmed by immunofluorescence confocal microscopy as well as by re-ChIP experiments (Figure 3E and F). In summary, these ex-



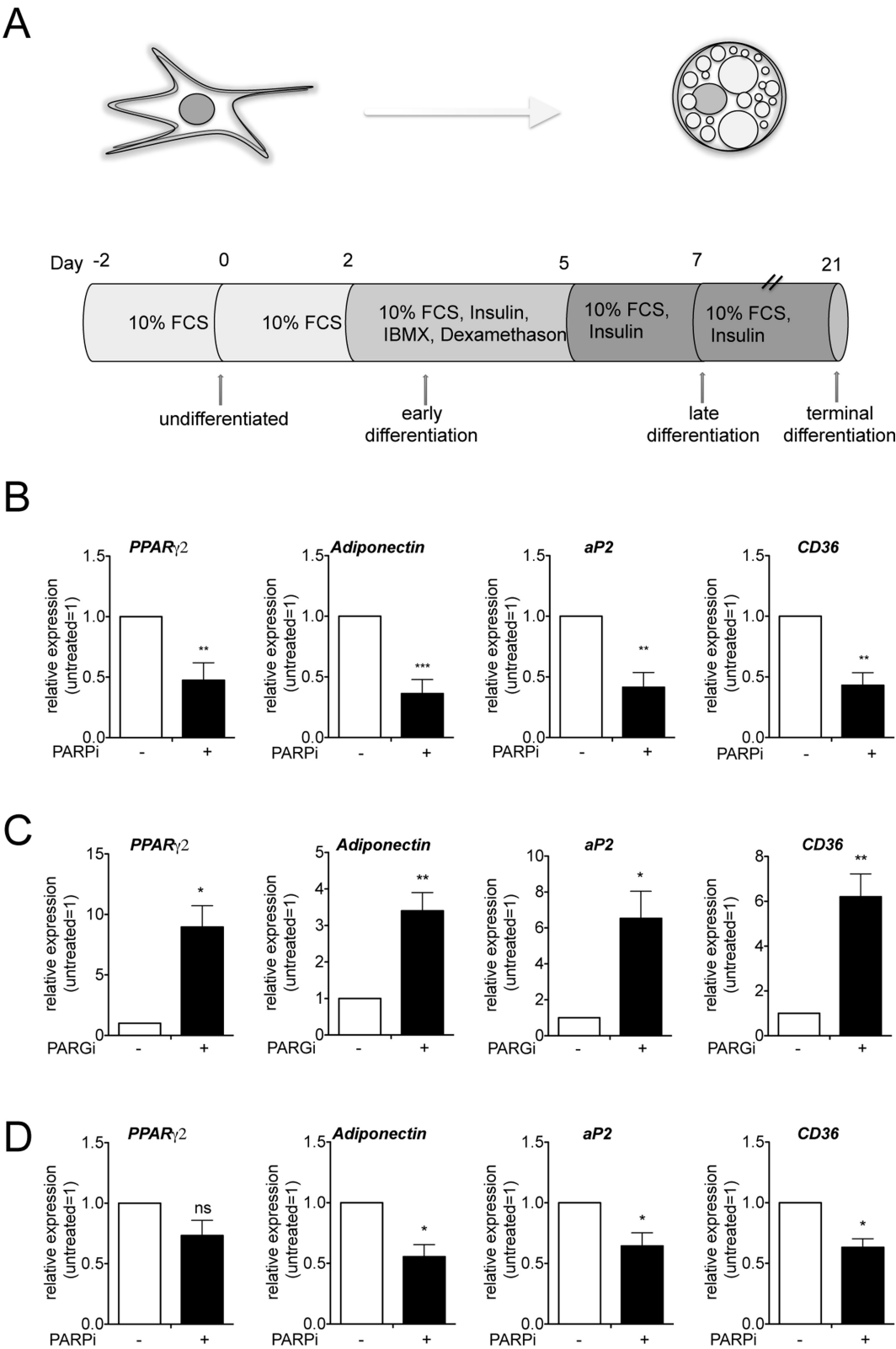


**Figure 2.** PAR formation is required for PPAR $\gamma$ -dependent gene expression. (A) Scheme of differentiation program: Adipogenesis was induced by adding insulin, 3-isobutyl-1-methylxanthine (IBMX) and dexamethasone for 3 days and maintaining cells in medium containing 10% FCS and insulin. (B) Cells were differentiated in the absence or presence of 10  $\mu$ M PARP inhibitor (PARPi, ABT888) (daily treatment) until day 7, at which point RNA was isolated ( $n = 8$ ). (C) Differentiating 3T3-L1 cells were left untreated or treated with 10  $\mu$ M PARG inhibitor (PARGi, RBPI-3) on days 1–5 and RNA was isolated on day 6 of differentiation ( $n = 5$ ). (D) Starting from day 7 of adipogenesis of 3T3-L1 cells, the culture medium containing insulin  $\pm$  10  $\mu$ M PARP inhibitor (PARPi, ABT888) was changed every second day. RNA was isolated at day 21 and gene expression was analyzed by RT-qPCR ( $n = 4$ ). All values represent the mean  $\pm$  SEM, untreated samples were set as 1. *t*-Test: \* $P < 0.05$ , \*\* $P < 0.01$ , \*\*\* $P < 0.001$ .

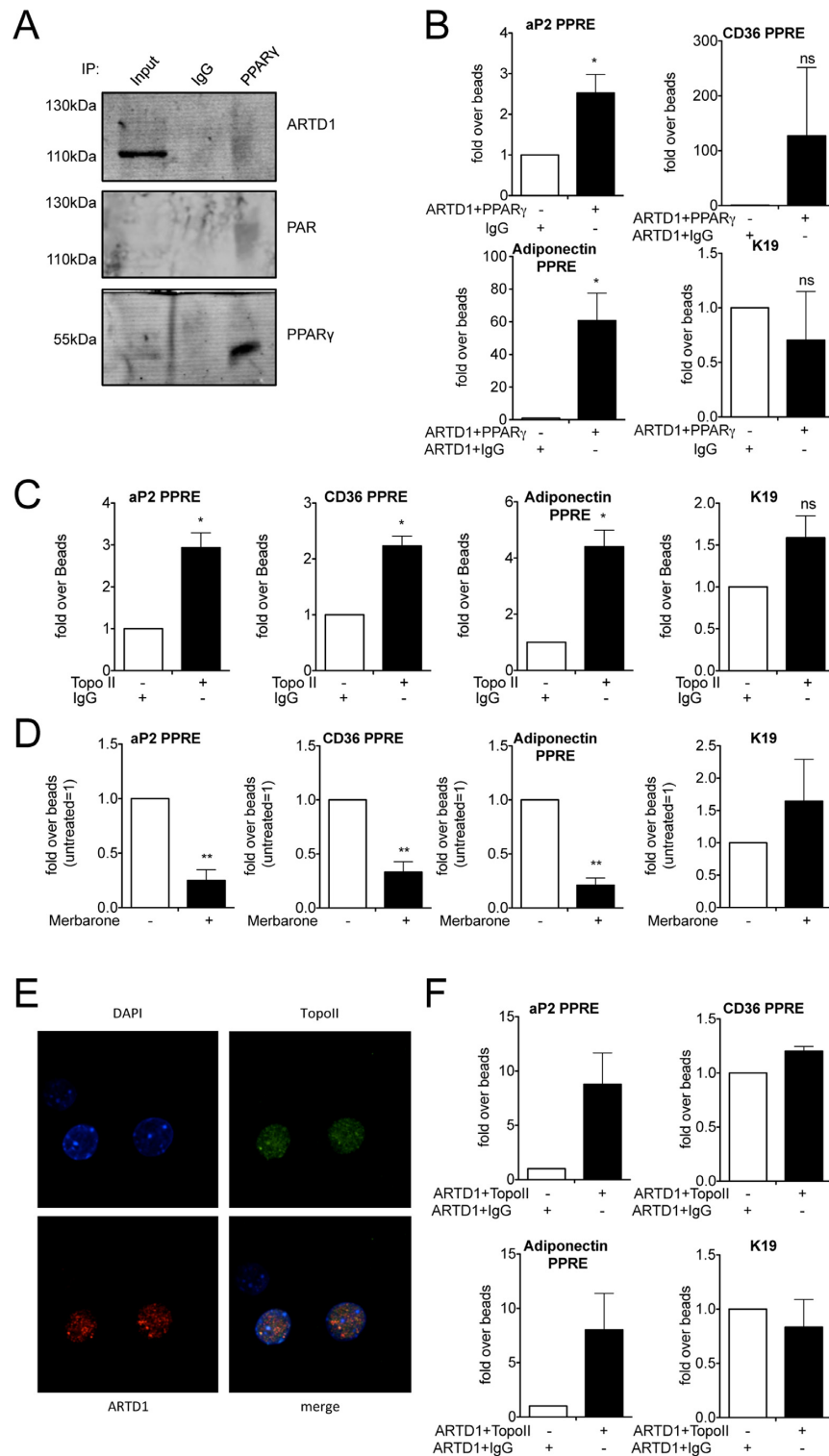


**Figure 3.** Ligand-dependent interaction of PPAR $\gamma$  and ARTD1 at the PPRES of PPAR $\gamma$ -target genes. (A) 3T3-L1 cells were differentiated until day 7, nuclear protein extracts were prepared and PPAR $\gamma$  was immunoprecipitated. To prevent degradation of PAR, extracts were treated with 10  $\mu$ M PARG inhibitor (RBPI-3). ChIP values were normalized over immunoglobulin G (IgG) control and over a control region (IL6 promoter). (B) ReChIP of ARTD1 and PPAR $\gamma$ . At day 7 of differentiation, cells were fixed and the chromatin was first precipitated with an ARTD1 antibody and then with a PPAR $\gamma$  antibody ( $n = 4$ ). (C) Cells were fixed at day 7 of differentiation and chromatin was immunoprecipitated with a topoisomerase II (TopoII) antibody ( $n = 3$ ). (D) Cells were treated with 50  $\mu$ M merbarone at days 5 and 6 and fixed at day 7 of differentiation and chromatin was immunoprecipitated with an ARTD1 antibody ( $n = 4$ ). (E) At day 7 of differentiation, 3T3-L1 cells were fixed with PFA and stained with an antibody against TopoII (green) and ARTD1 (red). DAPI was used to visualize the nuclei (blue). Cells were analyzed by confocal microscopy. (F) ReChIP of ARTD1 and TopoII. At day 7 of differentiation, cells were fixed and the chromatin was first precipitated with an ARTD1 antibody and then with a TopoII antibody ( $n = 4$ ). All values represent the mean  $\pm$  SEM. ChIP values were normalized over IgG control.  $t$ -test: \* $P < 0.05$ , \*\* $P < 0.01$ .



periments suggest that ARTD1 and PPAR $\gamma$  interact at the PPRES of target genes and that TopoII activity is required for the recruitment of ARTD1 to PPAR $\gamma$ -dependent genes.

### ARTD1 induces PAR formation at PPRES of adipogenic genes and increases the transcriptional potential of PPAR $\gamma$

To investigate if the PAR-polymers induced during differentiation are indeed present at the chromatin of PPRES of PPAR $\gamma$  target genes, an anti-PAR ChIP was performed. PAR was specifically enriched at the promoters of PPAR $\gamma$ -target genes, which increased during differentiation from day 0 to day 7 (Figure 4A), indicating that PAR is specifically formed at PPRES of adipogenic genes during differentiation. To gain further insight into the PAR-regulated transcriptional potential of PPAR $\gamma$ , we performed luciferase assays in the presence and absence of PARP inhibitor. Analysis of transcriptional activity of PPAR $\gamma$  in 3T3-L1 cells revealed that inhibition of PAR formation reduced both basal and rosiglitazone-induced PPAR $\gamma$  transcriptional activity (Figure 4B). In contrast, co-treating the cells with PARG inhibitor increased the response to rosiglitazone as compared to the untreated control (Figure 4C). Since overexpression of wt ARTD1, but not of the enzymatically inactive mutants E988K or Y907A/C908Y, enhanced the RLU Firefly/Renilla signal, PPAR $\gamma$ -dependent gene expression was clearly mediated by ARTD1-dependent PAR formation (Figure 4D). Similar results were obtained by using a different PARP inhibitor and when experiments were carried out in HEK 293T cells (Supplementary Figure S4A–C). To test whether induction of PAR formation by other means also enhances PPAR $\gamma$  activity, we used H<sub>2</sub>O<sub>2</sub> to induce PAR formation. Similar to ligand-induced PAR formation, treatment of cells with H<sub>2</sub>O<sub>2</sub> also enhanced complex formation between PPAR $\gamma$ 2 and ARTD1 in cells (Supplementary Figure S4D and E). H<sub>2</sub>O<sub>2</sub> treatment also increased luciferase activity to a level that was comparable to the effect induced by rosiglitazone (Figure 4E). Co-treatment with PARP inhibitor abolished this stimulation, indicating that PAR formation was indeed responsible for the observed effect. Co-treating the cells with PARG inhibitor enhanced the response to H<sub>2</sub>O<sub>2</sub> as compared to an inactive control substance (Figure 4F). Since overexpression of wt ARTD1 strongly enhanced the RLU Firefly/Renilla signal, while neither the E988K nor the Y907A/C908Y enzymatically inactive mutant conferred this effect, ARTD1-dependent PAR formation also contributed to the H<sub>2</sub>O<sub>2</sub>-induced increase in PPAR $\gamma$ -dependent gene expression (Figure 4G). A similar result was observed in HEK 293T cells overexpressing PPAR $\gamma$  and either one of the ARTD1 mutants (Supplementary Figure S4F). To analyze if this ARTD1-dependent increase in PPAR $\gamma$ -dependent gene expression was dependent on TopoII activity, the effect of merbarone on Luciferase activity upon rosiglitazone or H<sub>2</sub>O<sub>2</sub> stimulation was analyzed (S4G, S4H). As observed for the differentiating 3T3-L1 cells, TopoII activity was also required for PPAR $\gamma$ -dependent gene expression for this readout. To confirm that H<sub>2</sub>O<sub>2</sub>-induced PAR formation functionally regulates PPAR $\gamma$ -mediated transcriptional activation with a physiologically more relevant readout, the effect was studied in differentiating 3T3-L1 cells. Cells were treated with

H<sub>2</sub>O<sub>2</sub> in the presence or absence of PARP inhibitor at day 3 of differentiation. Two hours after treatment with H<sub>2</sub>O<sub>2</sub>, the expression of *aP2*, *CD36* and *adiponectin* was analyzed by qRT-PCR. H<sub>2</sub>O<sub>2</sub> treatment led to significantly increased expression of *adiponectin* in PPAR $\gamma$ -overexpressing 3T3-L1 cells, which was inhibited by PARP inhibitor treatment (Supplementary Figure S4J). Not all PPAR $\gamma$  target genes (e.g. *aP2*) were induced upon H<sub>2</sub>O<sub>2</sub> stimulation. These results demonstrate that H<sub>2</sub>O<sub>2</sub>-induced formation of PAR is sufficient to increase the expression of at least a subset of PPAR $\gamma$ -dependent genes.

### PAR formation controls PPAR $\gamma$ -dependent gene expression by enhancing ligand binding and facilitating ligand-induced co-factor exchange

Transcriptional activity of nuclear receptors, such as PPARs, is regulated by the dynamic exchange of co-activator and co-repressor complexes at the promoters of the target genes (11,12,36). Two of the most important regulators of PPAR $\gamma$  functions are the co-activator p300 and the co-repressor NCoR1 (37,38). To elucidate the role of PAR formation in the binding of PPAR $\gamma$  to its co-activator p300, GST pull-down experiments with recombinant ARTD1, p300 and PPAR $\gamma$  were performed. Under the tested conditions, rosiglitazone was poorly able to induce complex formation between PPAR $\gamma$  and p300 (Figure 5A). Addition of unmodified ARTD1 enhanced this formation in a rosiglitazone-dependent manner, which was even further enhanced, when automodified PARylated ARTD1 was added, but using the same concentration of rosiglitazone (Figure 5A), suggesting that ADP-ribosylated ARTD1 enhances PPAR $\gamma$  ligand binding and subsequent complex formation with p300. Indeed, addition of ADP-ribosylated ARTD1 enhanced binding of p300 even at a very low rosiglitazone concentration where no complex formation was observed in samples without ARTD1 or with non-modified ARTD1 (Supplementary Figure S5A). PPAR $\gamma$ /p300 complex formation was also enhanced by inducing ARTD1-dependent PAR formation *in vivo* by H<sub>2</sub>O<sub>2</sub> (Supplementary Figure S5B).

To further substantiate that automodified ARTD1 is able to enhance ligand binding to PPAR $\gamma$ 2, we took advantage of a ligand-binding assay employing <sup>3</sup>H-labeled rosiglitazone (Supplementary Figure S5C). Using recombinant full-length PPAR $\gamma$ 2, we detected specific ligand binding to PPAR $\gamma$ 2. This ligand binding was significantly enhanced when ADP-ribosylated ARTD1 was added to the binding reaction (Figure 5B). Unmodified ARTD1 (incubated without NAD<sup>+</sup> or using the inactive mutant Y907A/C908Y) did not show this increase, indicating that ADP-ribosylation of ARTD1 was responsible for this phenomenon. To test if also free PAR increases ligand binding, we supplemented the binding reaction with PAR only (Figure 5B). However, no increase in ligand binding was observed upon addition of free PAR, suggesting that it is indeed PAR covalently attached to ARTD1 that changes the ligand binding potential of PPAR $\gamma$ .

Next, we analyzed if recruitment of p300 co-activator to the PPAR $\gamma$ -dependent genes is regulated by PAR formation *in vivo*. In 3T3-L1 cells differentiated for 7 days,

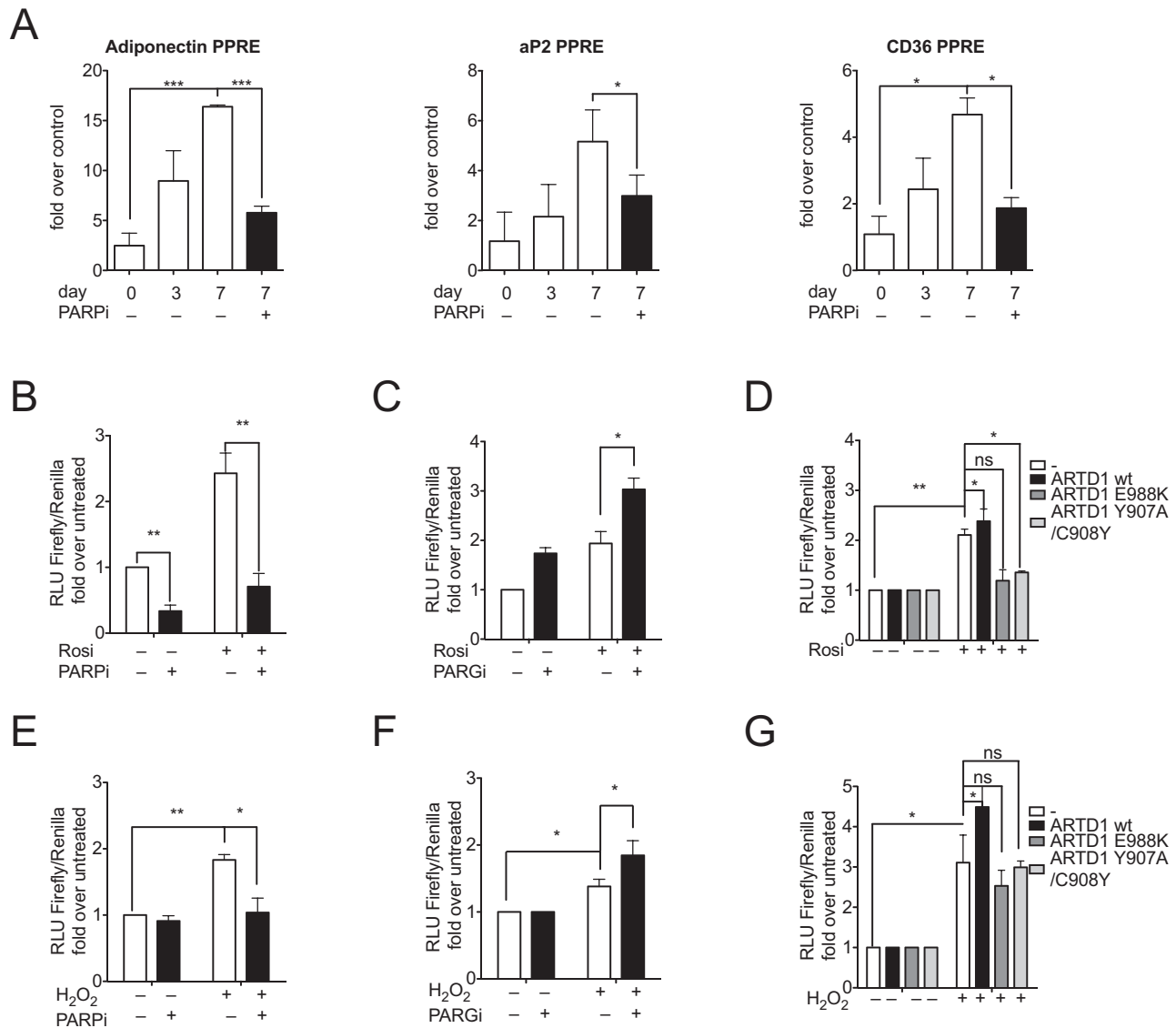


**Figure 4.** PAR formation enhances ligand binding to PPAR $\gamma$ . (A) 3T3-L1 cells were treated daily with 10  $\mu$ M PJ34 starting at day 1 or not. At day 0, 3 or 7, cells were fixed with formaldehyde and chromatin was precipitated with an anti-PAR antibody. Values were normalized over IgG and over IL-6-100 as control gene. (B) 3T3-L1 cells overexpressing PPAR $\gamma$ 2 were treated with 10  $\mu$ M rosiglitazone in the presence or absence of 10  $\mu$ M PARP inhibitor (PARPi, PJ34) for 16 h and luciferase activity was subsequently measured ( $n = 5$ ). (C) 3T3-L1 cells overexpressing PPAR $\gamma$ 2 were pretreated with 10  $\mu$ M PARG inhibitor (PARGi, RBPI-3) and treated with 10  $\mu$ M rosiglitazone for 16 h and luciferase activity was subsequently measured. (D) 3T3-L1 cells co-overexpressing PPAR $\gamma$ 2 and ARTD1 (wt,  $n = 5$ ), ARTD1 E988K ( $n = 7$ ), ARTD1 Y907A/C908Y ( $n = 3$ ) or GFP (as a negative control,  $n = 7$ ) were treated with 10  $\mu$ M rosiglitazone for 16 h in the presence or absence of 10  $\mu$ M (PARPi, PJ34) and luciferase activity was subsequently measured ( $n = 4$ ). (E) 3T3-L1 cells overexpressing PPAR $\gamma$ 2 were treated with 1 mM H<sub>2</sub>O<sub>2</sub> for 2 h in the presence of 30  $\mu$ M catalase inhibitor (3-AT) and in the presence or absence of 10  $\mu$ M PJ34. Luciferase activity was measured ( $n = 4$ ). (F) 3T3-L1 cells overexpressing PPAR $\gamma$ 2 were pretreated with 10  $\mu$ M PARG inhibitor (RBPI-3) and treated with 1 mM H<sub>2</sub>O<sub>2</sub> for 2 h in the presence of 30  $\mu$ M catalase inhibitor (3-AT) and luciferase activity was subsequently measured. (G) 3T3-L1 cells co-overexpressing PPAR $\gamma$ 2 and ARTD1 (wt,  $n = 5$ ), ARTD1 E988K ( $n = 4$ ), ARTD1 Y907A/C908Y ( $n = 3$ ) or GFP (as a negative control,  $n = 5$ ) were treated with 1 mM H<sub>2</sub>O<sub>2</sub> for 2 h in the presence of 30  $\mu$ M catalase inhibitor (3-AT). All values represent the mean  $\pm$  SEM;  $t$ -test: \* $P < 0.05$ , \*\* $P < 0.01$ , \*\*\* $P < 0.001$ .

binding of p300 to the PPRE of *aP2* and *adiponectin* was significantly reduced upon PARP inhibitor treatment (Figure 5C), suggesting that the reduction of p300 at the PPRE translates into reduced expression of the corresponding gene. The PPAR $\gamma$ -dependent gene *CD36* showed the same trend. Importantly, p300 binding was not changed upon PARP inhibitor treatment at the promoter of the PPAR $\gamma$ -independent control gene *K19*. Interestingly, and in agree-

ment with the respective co-activator and co-repressor functions, occupancy of the co-repressor NCoR-1 exhibited the opposite behavior and was increased at the PPRES of PPAR $\gamma$ -dependent genes upon PARP inhibitor treatment (Figure 5D). A similar result was obtained with cells that were treated with PARP inhibitor from day 5 to 8 of differentiation (Supplementary Figure S5D). Additionally, inhibition of TopoII activity, which is needed for PAR for-

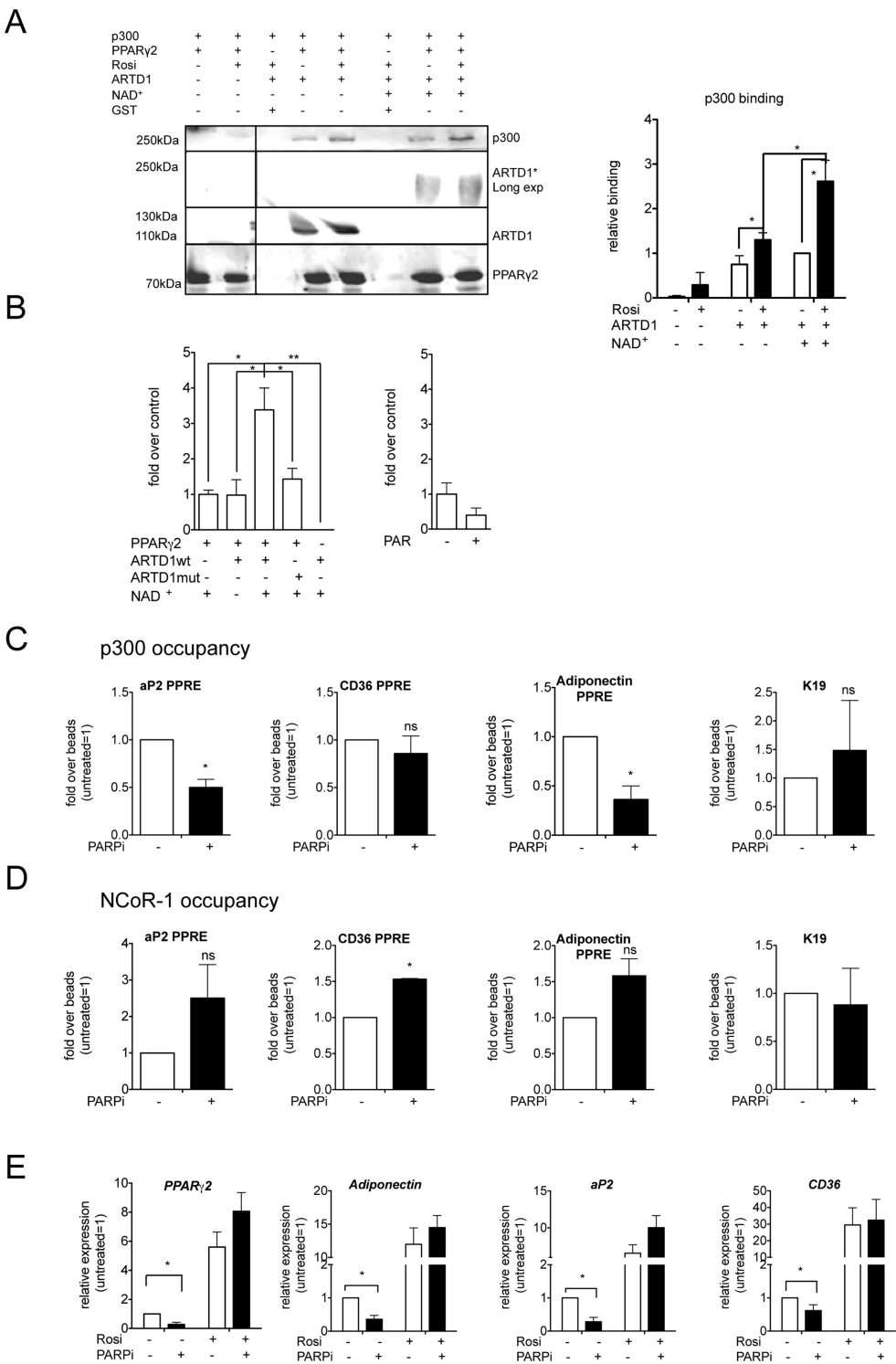


**Figure 5.** PAR formation controls PPAR $\gamma$ -dependent gene expression by promoting ligand induced cofactor exchange. (A) Left: PPAR $\gamma$ 2-GST pull-down of ARTD1 (without NAD $^{+}$  = unmodified, with NAD $^{+}$  = automodified; please note that modified ARTD1 has a higher molecular weight than unmodified ARTD1) and p300 in the presence or absence of 10  $\mu$ M rosiglitazone. Black line indicates the removal of lanes on the same blot that are not relevant for the experiment. Right: Quantification of p300 signal. Intensities were normalized against the corresponding PPAR $\gamma$  signal and then normalized against modified ARTD1 in the absence of rosiglitazone (= 1). Statistical analysis represents data from four independent experiments. (B) Radioligand binding assay in the presence of modified or unmodified ARTD1 (wt or mutant (Y907A, C908Y),  $\pm$ 100 nM NAD $^{+}$ ). Values show specific binding normalized to control (PPAR $\gamma$  without ARTD1, column 1) ( $n$  = 3–5). (C) Radioligand binding assay in the presence or absence of PAR. Values show specific binding normalized to control (PPAR $\gamma$  without ARTD1 ( $n$  = 3)). (D) Same analysis as in C for NCoR-1 ( $n$  = 3). (E) 3T3-L1 cells were treated with 10  $\mu$ M rosiglitazone or 10  $\mu$ M (PARPi, ABT888) or both at days 2–6 of adipogenesis ( $n$  = 4). All values represent the mean  $\pm$  SEM; ChIP values were normalized over IgG control.  $t$ -test: \* $P$  < 0.05, \*\* $P$  < 0.01.

mation, led to reduced p300 levels (Supplementary Figure S5E). If automodified ARTD1 is able to enhance PPAR $\gamma$  ligand binding and subsequently transcriptional co-factor exchange, then treating cells with a high dose of rosiglitazone should functionally compensate the repressory PARP inhibitor effect on PPAR $\gamma$ -dependent gene expression. Differentiating 3T3-L1 cells were therefore treated with PARP inhibitor or not and supplemented with an excess of rosiglitazone. The results of these experiments showed that an excess of rosiglitazone indeed overcomes the PARP inhibitor effect on *aP2*, *CD36*, *adiponectin* and *PPAR $\gamma$ 2* gene expression (Figure 5E). This effect was indeed mediated by p300, as treatment with PARP inhibitor in rosiglitazone-treated cells could not reduce p300 levels in contrast to cells that have not been treated with an excess PPAR $\gamma$  ligand and that showed reduced p300 binding upon PARP inhibitor treatment (Supplementary Figure S5F).

In summary, these findings show that ADP-ribosylated ARTD1 interacts with PPAR $\gamma$ , enhances ligand binding to PPAR $\gamma$  and thereby facilitates co-factor exchange, resulting in enhanced gene expression of PPAR $\gamma$  target genes and thus clarifies the mechanism by which ARTD1 promotes adipocyte differentiation and function.

## DISCUSSION

Adipogenesis is driven by changes in gene transcription, being reliant on the reprogramming of the cellular transcription profiles through the activation of specific transcription factors (39). Transcription factors that determine the early phase of adipogenesis, such as Stat5a, C/EBP- $\beta$  and C/EBP- $\delta$ , are required for the formation of so-called transcriptional hotspots that prime the chromatin for PPAR $\gamma$  binding (2). PPAR $\gamma$  is a ligand-gated transcription factor and its activity relies on transcriptional co-factors that regulate chromatin compaction and recruit elements of the transcription machinery (2,39). During the course of adipogenesis, co-repressors are replaced by co-activators, which induce a permissive chromatin state, thereby rendering the DNA accessible for the transcription machinery.

We have previously shown that ADP-ribosylation plays an important role in adipogenesis and adipocyte function (24,25). We have shown that ARTD1 activity is important for the late phase of adipogenic differentiation of 3T3-L1 cells and is likely regulated by the formation of transient, site-specific double-strand DNA breaks at promoters of PPAR $\gamma$ -dependent genes (24). This suggested that ARTD1 is not required for the formation of transcription factor hotspots but for sustained PPAR $\gamma$ -dependent gene expression. These initial findings were further corroborated by *in vivo* studies, showing that the presence of ARTD1 is necessary for efficient adipogenesis, whereas lack of ARTD1 limits adipocyte function, adipocyte size and lipid metabolism in the liver (25). Although these studies have established a role for ARTD1 in adipogenesis and adipocyte turnover, the molecular mechanism by which ARTD1, and more specifically its ADP-ribosylation, co-regulate these processes remained to be elucidated.

In the current study, we show that ARTD1-induced poly-ADP-ribosylation is an important mediator of WAT function and PPAR $\gamma$ -dependent gene expression in mice on

HFD. Furthermore, our work demonstrates that ARTD1-dependent ADP-ribosylation also influences adipogenic gene expression in cultured cells. Treating cells with an excess of PPAR $\gamma$  ligand overcame the repression of PPAR $\gamma$ -dependent gene expression by PARP inhibitor treatment, indicating that ADP-ribosylated ARTD1 stabilizes PPAR $\gamma$  ligand binding. These results define enhancement of ligand binding as the mechanism by which PAR formation regulates and promotes PPAR $\gamma$ -dependent gene expression in the later phase of adipogenesis and thus uncover a new regulatory mechanism of ARTD1-induced ADP-ribosylation for nuclear factor-regulated gene expression. Together, our results support a model in which TopoII-dependent torsional stress or DNA structures activate ARTD1. Modified ARTD1 interacts with PPAR $\gamma$  and stabilizes PPAR $\gamma$  ligand binding, which allows an exchange of the NCoR1 co-repressor with the p300 co-activator at the promoters of PPAR $\gamma$  target genes (Supplementary Figure S5G).

Interestingly, H<sub>2</sub>O<sub>2</sub>-induced PAR formation also enhanced PPAR $\gamma$ -dependent gene expression using a luciferase reporter assay or the analysis of endogenous PPAR $\gamma$  target genes. This observation suggests that H<sub>2</sub>O<sub>2</sub> signaling enhances gene expression specifically, possibly by inducing ADP-ribosylation to the promoters. Further investigations are required to study how a possible targeting of PAR formation by H<sub>2</sub>O<sub>2</sub> is regulated.

We show here that TopoII activity is required for recruitment and activation of ARTD1 at PPAR $\gamma$ -dependent genes. Although ARTD1 activation has been linked to TopoII activity (40), it was not clear yet if the TopoII activity is needed for the recruitment of ARTD1. Here, we show that TopoII activity is indeed required for ARTD1 recruitment and subsequent activation, a finding which supports a model where beginning transcription leads to the requirement of TopoII cleavage, thereby recruiting and activating ARTD1, which leads to increased gene expression. Since TopoII cleavage does not generate free DNA ends and does not activate or require DNA repair mechanisms (41), ADP-ribosylation at TopoII cleavage sites at PPAR $\gamma$ -dependent genes functions differently from the function of this enzyme in DNA repair. In addition, this means that ARTD1 is not activated by free DNA ends, but rather by DNA structures or torsional stress created during TopoII cleavage.

PPAR $\gamma$  is a ligand-dependent transcription factor, but the identity of the physiological ligands remains controversial and is under active investigation. During adipogenesis, 3T3-L1 cells synthesize a PPAR $\gamma$ -activating substance, but its identity remains elusive (42). Polyunsaturated fatty acids and related molecules can activate PPAR $\gamma$  in micromolar concentrations (43–46), but it is not yet known if the concentration inside the cell and in proximity to the receptor is sufficient to activate PPAR $\gamma$  or not (47). We demonstrate here that the increased presence of ARTD1-mediated ADP-ribosylation activates PPAR $\gamma$ -dependent gene expression and show direct binding and interaction of automodified ARTD1 with PPAR $\gamma$ , which increased ligand binding to PPAR $\gamma$  and in this way apparently increases ligand affinity. Interestingly, only ADP-ribosylated ARTD1 but not isolated PAR was able to enhance PPAR $\gamma$  ligand binding, suggesting that the positioning of the polymers in the protein context is impor-



tant. Although PPAR $\gamma$  can be ADP-ribosylated by ARTD1 *in vitro* and modified PPAR $\gamma$  has been described in cells (48), our data clearly show that the automodification of ARTD1 alone is sufficient to strongly enhance ligand binding to PPAR $\gamma$ . It remains to be clarified how automodified ARTD1 enhances binding of PPAR $\gamma$  ligand. One possibility is, that automodified ARTD1 adapts a different conformation compared to unmodified ARTD1, which subsequently induces a PPAR $\gamma$  conformation that facilitates ligand binding. Another possibility is that the conformation of PPAR $\gamma$  remains unchanged, but the interaction of modified ARTD1 with PPAR $\gamma$  positions the polymers in a way that they act like a cage, increasing the local ligand concentration and subsequently also PPAR $\gamma$ /ligand complex formation. The induction of PAR may thus sensitize cells in cases where endogenous PPAR $\gamma$  ligand concentrations are low and thereby facilitate PPAR $\gamma$ -dependent gene expression. Our results define ADP-ribosylated ARTD1 as a new modulator of PPAR $\gamma$  activity and that ARTD1-mediated ADP-ribosylation increases ligand functionality. This is the first study to our knowledge that shows that ADP-ribosylation of ARTD1 changes the properties of an interacting protein.

PPAR $\gamma$  antagonists exhibit gene-silencing activity due to their ability to promote the recruitment of co-repressors and the subsequent formation of a condensed chromatin state (49). Co-repressors, such as NCoR-1, are dislodged from PPAR $\gamma$  upon ligand binding and their inhibition has the potential to increase the expression of PPAR $\gamma$  target genes (13,50). In contrast, agonists favor the formation of co-activator complexes that acetylate histones and thereby induce chromatin de-condensation and transcriptional initiation (49). An important component of such co-activator complexes are the acetyltransferases p300/CBP, which interact with the N-terminus of PPAR $\gamma$  in a ligand-independent manner, whereas binding to the C-terminus is ligand-dependent (36). In the experimental system of adipogenesis studied here, PAR formation favored ligand binding and p300 recruitment to PPREs and thereby ensured continuous expression of PPAR $\gamma$  target genes. In contrast to this, ARTD1 protein, but not its enzymatic activity was required for full transcriptional activation of NF- $\kappa$ B in the presence of p300 (51), indicating that the regulatory mechanism underlying the control of PPAR $\gamma$ -dependent gene expression is different to the one described for NF- $\kappa$ B. Requirement of PAR for p300 recruitment is consistent with the model of PAR as a platform for the recruitment and binding of chromatin remodeling components and elements of the transcription machinery (52). Based on our results, we postulate that ARTD1 represents a new regulator of the PPAR $\gamma$  co-activator complex involved in promoting PPAR $\gamma$ -dependent gene expression during adipogenesis.

Different other nuclear receptors and transcription factors have been linked to TopoII- and ARTD1-dependent activation of gene expression, supporting the idea that this might be a general regulatory mechanism for different nuclear receptors involved in the regulation of various cellular processes (40,53,54). PPAR $\gamma$  is also expressed in cells of the immune system, such as macrophages, where it can act as a repressor for inflammatory gene expression through a process called transrepression (55). It is an intriguing possibility that PAR formation may also be involved in this pro-

cess. Recently, a role for NCoR1 in systemic insulin resistance upon HFD-induced obesity has been described (56), raising the question as to whether PAR formation might be important for the co-factor recruitment and thus for the development of insulin resistance in this context.

An interesting and unexpected result of this study was the strong effect of PARP inhibitor treatment on WAT formation and the inflammatory status in mice exposed to HFD. Adipocytes are known to secrete inflammatory mediators (30). However, since also macrophages infiltrate adipose tissue under conditions of obesity, the reduced adipose tissue inflammation observed in PARP inhibitor-treated mice could be mediated both by adipocytes and macrophages. Since scWAT is a potential target for therapies aimed at treating metabolic syndrome (57), PARP inhibitors may open up new treatment options for patients suffering from this disorder. Due to their high level of tolerance and anti-inflammatory effects, PARP inhibitors are considered to be promising therapeutic agents.

## SUPPLEMENTARY DATA

Supplementary Data are available at NAR Online.

## ACKNOWLEDGEMENTS

The RBPI-3 PARG inhibitor was a kind gift of Prof. Dr. Paul J. Hergenrother (University of Illinois, USA). The novel pan-PARP inhibitor MRL-45696 was kindly provided by Thomas Vogt (Merck Research Laboratories). We thank M. Altmeyer (NNF CPR, Copenhagen) for generating the inactive ARTD1 mutant (Y907A/C908Y), Laia Morato (EPFL, Switzerland) for help with ART activity measurements, and C. Wolfrum for the 3T3-L1 cells and for helpful discussions (ETH Zurich, Switzerland). W. Wahli (University of Lausanne) provided the luciferase and PPAR $\gamma$  expression plasmids. We thank Florian Freimoser, Stephan Christen and all other members of the Institute of Veterinary Biochemistry and Molecular Biology (University of Zurich, Switzerland) for help and discussions during the preparation of this manuscript.

*Authors Contributions:* M.L. planned and performed the experiments, evaluated the data and wrote the manuscript. M.L., A.M. and P.J.R. performed histological and RNA isolation from mouse tissue. M.L. and F.K. analyzed gene expression in adipose tissue. E.P. organized and performed mouse studies and performed measurements of total ART activity in mouse tissue. J.A. supervised experiments and revised the manuscript. M.O.H. supervised the study and wrote the manuscript.

Johan Auwerx is a founder and SAB member of Mitokyne.

## FUNDING

Forschungskredit of the University of Zurich [to M.L.]; Academy of Finland, Saastamoinen Foundation, Finnish Cultural Foundation and Finnish Diabetes Foundation [to E.P.]; Ecole Polytechnique Fédérale de Lausanne, the EU Ideas [AdG-23138 'Sirtuins'], Swiss National Science Foundation [31003A-124713 to J.A.]; Kanton of Zurich, Swiss National Science Foundation [310030B-138667 and

310030-157019 to M.O.H.]. Funding for open access charge: Forschungskredit of the University of Zurich [to M.L.]; Swiss National Science Foundation [31003A-124713 to J.A.].

*Conflict of interest statement.* None declared.

## REFERENCES

- Church, C., Horowitz, M. and Rodeheffer, M. (2012) WAT is a functional adipocyte? *Adipocyte*, **1**, 38–45.
- Siersbaek, R., Nielsen, R., John, S., Sung, M.H., Baek, S., Loft, A., Hager, G.L. and Mandrup, S. (2011) Extensive chromatin remodelling and establishment of transcription factor 'hotspots' during early adipogenesis. *EMBO J.*, **30**, 1459–1472.
- Heikkinen, S., Auwerx, J. and Argmann, C.A. (2007) PPARgamma in human and mouse physiology. *Biochim. Biophys. Acta*, **1771**, 999–1013.
- Tontonoz, P. and Spiegelman, B.M. (2008) Fat and beyond: the diverse biology of PPAR $\gamma$ . *Annu. Rev. Biochem.*, **77**, 289–312.
- Vidal-Puig, A., Jimenez-Linan, M., Lowell, B.B., Hamann, A., Hu, E., Spiegelman, B., Flier, J.S. and Moller, D.E. (1996) Regulation of PPAR gamma gene expression by nutrition and obesity in rodents. *J. Clin. Invest.*, **97**, 2553–2561.
- Fajas, L., Auboeuf, D., Raspe, E., Schoonjans, K., Lefebvre, A.M., Saladin, R., Najib, J., Laville, M., Fruchart, J.C., Deeb, S. *et al.* (1997) The organization, promoter analysis, and expression of the human PPARgamma gene. *J. Biol. Chem.*, **272**, 18779–18789.
- Kliwer, S.A., Umehono, K., Mangelsdorf, D.J. and Evans, R.M. (1992) Retinoid X receptor interacts with nuclear receptors in retinoic acid, thyroid hormone and vitamin D3 signalling. *Nature*, **355**, 446–449.
- Escher, P., Braissant, O., Basu-Modak, S., Michalik, L., Wahli, W. and Desvergne, B. (2001) Rat PPARs: quantitative analysis in adult rat tissues and regulation in fasting and refeeding. *Endocrinology*, **142**, 4195–4202.
- Chawla, A., Boisvert, W.A., Lee, C.H., Laffitte, B.A., Barak, Y., Joseph, S.B., Liao, D., Nagy, L., Edwards, P.A., Curtiss, L.K. *et al.* (2001) A PPAR gamma-LXR-ABCA1 pathway in macrophages is involved in cholesterol efflux and atherogenesis. *Mol. Cell*, **7**, 161–171.
- Siersbaek, R., Nielsen, R. and Mandrup, S. (2010) PPAR $\gamma$  in adipocyte differentiation and metabolism - novel insights from genome-wide studies. *FEBS Lett.*, **584**, 3242–3249.
- Gampe, R.T. Jr., Montana, V.G., Lambert, M.H., Miller, A.B., Bledsoe, R.K., Milburn, M.V., Kliwer, S.A., Willson, T.M. and Xu, H.E. (2000) Asymmetry in the PPAR $\gamma$ /RXR $\alpha$  crystal structure reveals the molecular basis of heterodimerization among nuclear receptors. *Mol. Cell*, **5**, 545–555.
- Kallenberger, B.C., Love, J.D., Chatterjee, V.K. and Schwabe, J.W. (2003) A dynamic mechanism of nuclear receptor activation and its perturbation in a human disease. *Nat. Struct. Biol.*, **10**, 136–140.
- Yu, C., Markan, K., Temple, K.A., Deplewski, D., Brady, M.J. and Cohen, R.N. (2005) The nuclear receptor corepressors NCoR and SMRT decrease peroxisome proliferator-activated receptor gamma transcriptional activity and repress 3T3-L1 adipogenesis. *J. Biol. Chem.*, **280**, 13600–13605.
- Tontonoz, P., Hu, E., Graves, R.A., Budavari, A.I. and Spiegelman, B.M. (1994) mPPAR gamma 2: tissue-specific regulator of an adipocyte enhancer. *Genes Dev.*, **8**, 1224–1234.
- Leferova, M.I., Zhang, Y., Steger, D.J., Schupp, M., Schug, J., Cristancho, A., Feng, D., Zhuo, D., Stoekert, C.J. Jr., Liu, X.S. *et al.* (2008) PPAR $\gamma$  and C/EBP factors orchestrate adipocyte biology via adjacent binding on a genome-wide scale. *Genes Dev.*, **22**, 2941–2952.
- Saladin, R., Fajas, L., Dana, S., Halvorsen, Y.D., Auwerx, J. and Briggs, M. (1999) Differential regulation of peroxisome proliferator activated receptor gamma1 (PPARgamma1) and PPARgamma2 messenger RNA expression in the early stages of adipogenesis. *Cell Growth Differ.*, **10**, 43–48.
- Rosen, E.D., Hsu, C.H., Wang, X., Sakai, S., Freeman, M.W., Gonzalez, F.J. and Spiegelman, B.M. (2002) C/EBPalpha induces adipogenesis through PPARgamma: a unified pathway. *Genes Dev.*, **16**, 22–26.
- Hottiger, M.O., Hassa, P.O., Luscher, B., Schuler, H. and Koch-Nolte, F. (2010) Toward a unified nomenclature for mammalian ADP-ribosyltransferases. *Trends Biochem. Sci.*, **35**, 208–219.
- Vyas, S., Matic, I., Uchima, L., Rood, J., Zaja, R., Hay, R.T., Ahel, I. and Chang, P. (2014) Family-wide analysis of poly(ADP-ribose) polymerase activity. *Nat. Commun.*, **5**, 4426.
- Hassa, P.O. and Hottiger, M.O. (2008) The diverse biological roles of mammalian PARPs, a small but powerful family of poly-ADP-ribose polymerases. *Front. Biosci.*, **13**, 3046–3082.
- Graziani, G. and Szabo, C. (2005) Clinical perspectives of PARP inhibitors. *Pharmacol. Res.*, **52**, 109–118.
- Underhill, C., Toulmonde, M. and Bonnefoi, H. (2011) A review of PARP inhibitors: from bench to bedside. *Ann. Oncol.*, **22**, 268–279.
- Wahlberg, E., Karlberg, T., Kouznetsova, E., Markova, N., Macchiarulo, A., Thorsell, A.G., Pol, E., Frostell, A., Ekblad, T., Oncu, D. *et al.* (2012) Family-wide chemical profiling and structural analysis of PARP and tankyrase inhibitors. *Nat. Biotechnol.*, **30**, 283–288.
- Erener, S., Hesse, M., Kostadinova, R. and Hottiger, M.O. (2012) Poly(ADP-ribose)polymerase-1 (PARP1) controls adipogenic gene expression and adipocyte function. *Mol. Endocrinol.*, **26**, 79–86.
- Erener, S., Mirsaidi, A., Hesse, M., Tiaden, A.N., Ellingsgaard, H., Kostadinova, R., Donath, M.Y., Richards, P.J. and Hottiger, M.O. (2012) ARTD1 deletion causes increased hepatic lipid accumulation in mice fed a high-fat diet and impairs adipocyte function and differentiation. *FASEB J.*, **26**, 2631–2638.
- Pirinen, E., Canto, C., Jo, Y.S., Morato, L., Zhang, H., Menzies, K.J., Williams, E.G., Mouchiroud, L., Moullan, N., Hagberg, C. *et al.* (2014) Pharmacological inhibition of poly(ADP-ribose) polymerases improves fitness and mitochondrial function in skeletal muscle. *Cell Metab.*, **19**, 1034–1041.
- Santoro, R., Li, J. and Grummt, I. (2002) The nucleolar remodeling complex NoRC mediates heterochromatin formation and silencing of ribosomal gene transcription. *Nat. Genet.*, **32**, 393–396.
- Bai, P. and Canto, C. (2012) The role of PARP-1 and PARP-2 enzymes in metabolic regulation and disease. *Cell Metab.*, **16**, 290–295.
- Bai, P., Houten, S.M., Huber, A., Schreiber, V., Watanabe, M., Kiss, B., de Murcia, G., Auwerx, J. and Menissier-de Murcia, J. (2007) Poly(ADP-ribose) polymerase-2 [corrected] controls adipocyte differentiation and adipose tissue function through the regulation of the activity of the retinoid X receptor/peroxisome proliferator-activated receptor-gamma [corrected] heterodimer. *J. Biol. Chem.*, **282**, 37738–37746.
- Skurk, T., Alberti-Huber, C., Herder, C. and Hauner, H. (2007) Relationship between adipocyte size and adipokine expression and secretion. *J. Clin. Endocrinol. Metab.*, **92**, 1023–1033.
- Després, J.-P. and Lemieux, I. (2006) Abdominal obesity and metabolic syndrome. *Nature*, **444**, 881–887.
- Ntambi, J.M. and Young-Cheul, K. (2000) Adipocyte differentiation and gene expression. *J. Nutr.*, **130**, 3122S–3126S.
- Picard, F., Kurtev, M., Chung, N., Topark-Ngarm, A., Senawong, T., Machado De Oliveira, R., Leid, M., McBurney, M.W. and Guarente, L. (2004) Sirt1 promotes fat mobilization in white adipocytes by repressing PPAR-gamma. *Nature*, **429**, 771–776.
- Shieh, W., Amé, J., Wilson, M., Wang, Z., Koh, D., Jacobson, M. and Jacobson, E. (1998) Poly(ADP-ribose) polymerase null mouse cells synthesize ADP-ribose polymers. *J. Biol. Chem.*, **273**, 30069–30072.
- Tee, M.K., Rogatsky, I., Tzagarakis-Foster, C., Cvoro, A., An, J., Christy, R.J., Yamamoto, K.R. and Leitman, D.C. (2004) Estradiol and selective estrogen receptor modulators differentially regulate target genes with estrogen receptors alpha and beta. *Mol. Biol. Cell*, **15**, 1262–1272.
- Gelman, L., Zhou, G., Fajas, L., Raspe, E., Fruchart, J.C. and Auwerx, J. (1999) p300 interacts with the N- and C-terminal part of PPARgamma2 in a ligand-independent and -dependent manner, respectively. *J. Biol. Chem.*, **274**, 7681–7688.
- Lee, J.W., Lee, Y.C., Na, S.Y., Jung, D.J. and Lee, S.K. (2001) Transcriptional coregulators of the nuclear receptor superfamily: coactivators and corepressors. *Cell. Mol. Life Sci.*, **58**, 289–297.
- Rosenfeld, M., Lunyak, V. and Glass, C. (2006) Sensors and signals: a coactivator/corepressor/epigenetic code for integrating signal-dependent programs of transcriptional response. *Genes Dev.*, **20**, 1405–1428.
- Rosen, E.D., Walkey, C.J., Puigserver, P. and Spiegelman, B.M. (2000) Transcriptional regulation of adipogenesis. *Genes Dev.*, **14**, 1293–1307.

40. Ju, B.-G., Lunyak, V., Perissi, V., Garcia-Bassets, I., Rose, D., Glass, C. and Rosenfeld, M. (2006) A topoisomerase II $\beta$ -mediated dsDNA break required for regulated transcription. *Science*, **312**, 1798–1802.
41. Nitiss, J.L. (2009) DNA topoisomerase II and its growing repertoire of biological functions. *Nat. Rev. Cancer*, **9**, 327–337.
42. Tzameli, I., Fang, H., Ollero, M., Shi, H., Hamm, J.K., Kievit, P., Hollenberg, A.N. and Flier, J.S. (2004) Regulated production of a peroxisome proliferator-activated receptor- $\gamma$  ligand during an early phase of adipocyte differentiation in 3T3-L1 adipocytes. *J. Biol. Chem.*, **279**, 36093–36102.
43. Forman, B.M., Chen, J. and Evans, R.M. (1997) Hypolipidemic drugs, polyunsaturated fatty acids, and eicosanoids are ligands for peroxisome proliferator-activated receptors  $\alpha$  and  $\delta$ . *Proc. Natl. Acad. Sci. U.S.A.*, **94**, 4312–4317.
44. Keller, H., Dreyer, C., Medin, J., Mahfoudi, A., Ozato, K. and Wahli, W. (1993) Fatty acids and retinoids control lipid metabolism through activation of peroxisome proliferator-activated receptor-retinoid X receptor heterodimers. *Proc. Natl. Acad. Sci. U.S.A.*, **90**, 2160–2164.
45. Kliewer, S.A., Sundseth, S.S., Jones, S.A., Brown, P.J., Wisely, G.B., Koble, C.S., Devchand, P., Wahli, W., Willson, T.M., Lenhard, J.M. *et al.* (1997) Fatty acids and eicosanoids regulate gene expression through direct interactions with peroxisome proliferator-activated receptors  $\alpha$  and  $\gamma$ . *Proc. Natl. Acad. Sci. U.S.A.*, **94**, 4318–4323.
46. Krey, G., Braissant, O., L'Horsset, F., Kalkhoven, E., Perroud, M., Parker, M.G. and Wahli, W. (1997) Fatty acids, eicosanoids, and hypolipidemic agents identified as ligands of peroxisome proliferator-activated receptors by coactivator-dependent receptor ligand assay. *Mol. Endocrinol.*, **11**, 779–791.
47. Houseknecht, K.L., Cole, B.M. and Steele, P.J. (2002) Peroxisome proliferator-activated receptor  $\gamma$  (PPAR $\gamma$ ) and its ligands: a review. *Domest. Anim. Endocrinol.*, **22**, 1–23.
48. Huang, D., Yang, C., Wang, Y., Liao, Y. and Huang, K. (2009) PARP-1 suppresses adiponectin expression through poly(ADP-ribosylation) of PPAR  $\gamma$  in cardiac fibroblasts. *Cardiovasc. Res.*, **81**, 98–107.
49. Bourguet, W., Germain, P. and Gronemeyer, H. (2000) Nuclear receptor ligand-binding domains: three-dimensional structures, molecular interactions and pharmacological implications. *Trends Pharmacol. Sci.*, **21**, 381–388.
50. Li, P., Fan, W., Xu, J., Lu, M., Yamamoto, H., Auwerx, J., Sears, D.D., Talukdar, S., Oh, D., Chen, A. *et al.* (2011) Adipocyte NCoR knockout decreases PPAR $\gamma$  phosphorylation and enhances PPAR $\gamma$  activity and insulin sensitivity. *Cell*, **147**, 815–826.
51. Hassa, P.O., Buerki, C., Lombardi, C., Imhof, R. and Hottiger, M.O. (2003) Transcriptional coactivation of nuclear factor- $\kappa$ B-dependent gene expression by p300 is regulated by poly(ADP)-ribose polymerase-1. *J. Biol. Chem.*, **278**, 45145–45153.
52. Tulin, A. and Spradling, A. (2003) Chromatin loosening by poly(ADP)-ribose polymerase (PARP) at *Drosophila* puff loci. *Science*, **299**, 560–562.
53. Ju, B.-G., Solum, D., Song, E., Lee, K.-J., Rose, D., Glass, C. and Rosenfeld, M. (2004) Activating the PARP-1 sensor component of the groucho/TLE1 corepressor complex mediates a CaMK kinase II $\delta$ -dependent neurogenic gene activation pathway. *Cell*, **119**, 815–829.
54. Ju, B.-G. and Rosenfeld, M. (2006) A breaking strategy for topoisomerase II $\beta$ /PARP-1-dependent regulated transcription. *Cell Cycle*, **5**, 2557–2560.
55. Straus, D.S. and Glass, C.K. (2007) Anti-inflammatory actions of PPAR ligands: new insights on cellular and molecular mechanisms. *Trends Immunol.*, **28**, 551–558.
56. Li, P., Spann, N.J., Kaikkonen, M.U., Lu, M., Oh da, Y., Fox, J.N., Bandyopadhyay, G., Talukdar, S., Xu, J., Lagakos, W.S. *et al.* (2013) NCoR repression of LXRs restricts macrophage biosynthesis of insulin-sensitizing omega 3 fatty acids. *Cell*, **155**, 200–214.
57. Rodriguez, A., Catalan, V., Gomez-Ambrosi, J. and Fruhbeck, G. (2007) Visceral and subcutaneous adiposity: are both potential therapeutic targets for tackling the metabolic syndrome? *Curr. Pharm. Des.*, **13**, 2169–2175.